

Detection of H I Associated with the Sculptor Dwarf Spheroidal Galaxy

Claude Carignan

Département de physique and Observatoire du mont Mégantic, Université de Montréal, C.P. 6128, Succ. centre ville, Montréal, Québec, Canada. H3C 3J7
e-mail: carignan@astro.umontreal.ca

Sylvie Beaulieu

Institute of Astronomy, University of Cambridge, Madingley Road, Cambridge, England. CB3 0HA
e-mail: beaulieu@ast.cam.ac.uk

Stéphanie Côté

Dominion Astrophysical Observatory, Herzberg Institute of Astrophysics, National Research Council of Canada, 5071 West Saanich Rd., Victoria, BC, Canada. V8X 4M6
e-mail: Stephanie.Cote@hia.nrc.ca

Serge Demers

Département de physique and Observatoire du mont Mégantic, Université de Montréal, C.P. 6128, Succ. centre ville, Montréal, Québec, Canada. H3C 3J7
e-mail: demers@astro.umontreal.ca

Mario Mateo

Departement of Astronomy, University of Michigan, 821 Dennison Bldg., Ann Arbor, MI 48109-1090, USA.
e-mail: mateo@ra.astro.lsa.umich.edu

ABSTRACT

Neutral hydrogen (H I) has been detected in the Local Group dwarf spheroidal galaxy Sculptor with the 64 m Parkes single dish and mapped with the Australia Telescope synthesis array. Most of the detected H I is in two clouds $\sim 15' - 20'$ away from the optical center. The gas is observed at the same systemic velocity than the stars but at ≥ 125 km s^{-1} away from the Magellanic Stream components in that region. A lower limit to the H I mass of $3.0 \times 10^4 \text{ M}_\odot$ is derived from the synthesis observation for an $(\mathcal{M}_{HI}/L_B) \simeq 0.02$. This amount of H I is compatible with mass loss expected from normal giants even if only 10% of the gas is retained by the galaxy in its neutral form.

Subject headings: galaxies: dwarf — galaxies: individual (Sculptor)
— Local Group — ISM: H I — techniques: interferometric

1. INTRODUCTION

It is generally believed that the dwarf spheroidal companions of the Galaxy and of M31 are completely devoid of a detectable interstellar medium (ISM), and in particular neutral hydrogen (eg Da Costa 1994). Previous attempts to detect H I in these galaxies (Knapp et al 1978; Mould et al 1990; Koribalsky et al 1994) have been carried out with the NRAO 91m, NRAO 41m and the Parkes 64m single dish telescopes; these studies were only able to set upper limits of $\sim 10^2 - 10^5 M_{\odot}$ for the H I content of eight of the nine dSph companions of the Milky Way. Thuan and Martin (1979) set limits on the H I content of two of the lower luminosity dSph systems near M 31 (And I and And III).

The only ambiguous detection near the Milky Way was the Sculptor dSph system. Knapp et al (1978; their figure 1) identified H I while observing Sculptor; they noted that

“... it is therefore (remotely) possible that the galaxy is embedded in the gas cloud at $+120 \text{ km s}^{-1}$.”,

In the end, they dismissed this possibility because the optical velocity of Sculptor was believed to be $\sim 200 \text{ km s}^{-1}$ at that time. Subsequent optical radial velocity studies of individual stars in Sculptor have shown its systemic velocity to be $\sim 110 \text{ km s}^{-1}$ (Queloz et al 1995), quite close to the H I velocity reported by Knapp et al (1978). Hence, in retrospect it appears that Sculptor was the first dSph system in which neutral gas was detected; however, because of the initial suggestion that the H I was not associated with the galaxy, this result has been largely forgotten.

The ISM of dSph and dSph-like systems may be considerably more complex than generally believed (see Mateo 1998 for a more extensive discussion). Johnson and Gottesman (1993) and Young and Lo (1997a) found complex H I distributions associated with the more luminous dSph-like M 31 systems, NGC 185 and NGC 205. In each case, the gas is distributed asymmetrically about the optical galaxy. 21-cm detections have also been reported in the remote Phoenix galaxy (Carignan, Demers & Côté 1991), a system sometimes mentioned as a transition system between dwarf irregular (dIrr) and dSph galaxies (van de Rydt et al 1991; van den Bergh 1994). Oosterloo et al. (1996) found an H I cloud near the even more remote Tucana dSph galaxy, but concluded that the

gas is more likely a high-velocity cloud (HVC) associated with the Magellanic Stream (MS); this will remain speculative until an optical radial velocity for this galaxy is obtained.

Sculptor is one of the closest of the Milky Way satellites at a distance of 88 kpc (Kaluzny et al 1995). Its angular size ($40'$) is comparable to that of the apparently largest dSph system (after Sagittarius), Fornax. The distribution of stars along the horizontal branch (HB) and the observed mean metallicity of Sculptor imply that the bulk of the stars in the galaxy have ages similar to that of the relatively young globular clusters found in the outer halo (Kaluzny et al 1995). The existing color-magnitude diagrams (CMD) do not reveal a strong intermediate age population (Da Costa 1984; Aaronson 1986), contrary to what is seen in Fornax or Carina (Stetson 1997; Hurley-Keller et al 1998). In contrast, the substantial spread in metallicity seen in Sculptor (Da Costa 1988, Kaluzny et al 1995) suggests that its star-formation (SF) history may have been rather complex. Da Costa (1984) and Grebel et al (1994) have noted a significant number of blue stars above Sculptor’s main sequence turn-off. While Da Costa identified them as blue stragglers, it is quite possible that these stars represent a small but significant younger population. Grebel et al (1994) argue strongly that a second SF episode has occurred in Sculptor, possibly triggered by the external accretion or internal accumulation of gas.

The radial velocity of Sculptor has been established by Queloz et al (1995) to be $109.9 \pm 1.4 \text{ km s}^{-1}$, confirming previous determinations of $109.2 \pm 4.5 \text{ km s}^{-1}$ by Aaronson & Olszewski (1987) and of $107.4 \pm 2.0 \text{ km s}^{-1}$ by Armandroff & Da Costa (1986). The velocity dispersion, derived from their sample of 23 K giants was found to be $6.2 \pm 1.1 \text{ km s}^{-1}$, for a global mass-to-light ratio $\sim 9 \pm 6 (M/Lv)_{\odot}$. The physical parameters of Sculptor are summarized in Table 1.

There is ample, growing evidence that other galaxies in the Local Group exhibit complex SF histories, but the relationship to their ISM remains unclear (eg, see Mateo 1998). As noted, Carina and Fornax have complex SF histories, but no detected ISM. Three more distant and isolated objects, Phoenix ($d \leq 400 \text{ kpc}$), Tucana ($d \leq 900 \text{ kpc}$), and Antlia ($d \simeq 1.15 \pm 0.1 \text{ Mpc}$) share many of the properties of the *bona fide* dSph systems. However, photometric studies (Canterna and Flower, 1977; Ortolani and Gratton, 1988; van de Rydt et al 1991; Whiting et

al 1997) have shown that Phoenix and Antlia possess stellar populations that seem to share properties of the populations found in both dSph and dIrr galaxies.

The growing evidence of complex SF histories in virtually all dwarf galaxies, including those with little or no detectable ISM, suggest that we do not yet understand the relationship between the stellar and gaseous components of these deceptively simple-looking systems (Mateo 1998). Because Sculptor is so close and because of its past (though unappreciated) detection at 21-cm, we have obtained new H I observations of the galaxy to study its ISM component in more detail. The new radio observations are described in Section 2; these include single dish H I observations using the Parkes 64m telescope, synthesis H I mapping done with the Narrabri Australia Telescope Compact Array (ATCA), and CO observations obtained with the Swedish-ESO Submillimeter Telescope (SEST) in Chile. In Section 3 we analyze in detail the content and distribution of the H I gas mapped with the ATCA, while in Section 4 we speculate about the possible origin of the detected gas in Sculptor. We end with a summary of our principal results and our main conclusions in Section 5.

2. OBSERVATIONS

2.1. Single Dish Parkes Observations

We observed Sculptor with the Parkes 64 m single dish telescope (Table 2) to confirm the detection reported by Knapp et al (1978). These new data were obtained in January 1992. The flux calibrator PKS 1934–638 was used to measure a mean system temperature during the run of $T_{sys} \simeq 50$ K with a HPBW of 14.9 ± 0.2 . The 8 MHz bandwidth, centered at 300 km s^{-1} , was divided in 1024 channels for a channel width of 1.65 km s^{-1} and a full velocity coverage of $[-544, 1144] \text{ km s}^{-1}$.

A total of 100 minutes integration was accumulated on Sculptor which, after averaging the 12 individual 500 second observations, resulted in a spectrum with an RMS noise of 0.013 Jy. This sets a 3σ detection limit of $\sim 100 \text{ } M_{\odot}$ at the distance of Sculptor. As we discuss in more detail below, we obtained a clear, strong detection of Sculptor with these observations. In addition to Sculptor, we also obtained new observations of the relatively recently discovered Sextans dSph (Irwin et al 1990). Contrary to the Sculptor observations, we did not detect H I towards Sextans.

Our 3σ upper limit for the neutral hydrogen content is $130 \text{ } M_{\odot}$ for any gas that might be located within the Parkes beam. For both galaxies, the Parkes telescope was centered directly on the optical centroids of the galaxies during these observations.

2.2. ATCA Synthesis Mapping

After confirming the earlier H I detection by Knapp et al (1978), we decided to try to map Sculptor with the 375m configuration of the ATCA on 1992 October 2 (Table 3). For these observations we obtained a total of 8.2 hours of integration on source, in blocks of 35 minutes and separated by 5 minute integrations of PKS 0042–442 for phase and amplitude calibration purposes. The absolute intensity scale was set by a 30 minutes observation of PKS 0407–658, which we assumed to have a flux density of 14.4 Jy at our observing frequency. Normally, the full array is comprised of six antennae; however, data from the 6th antenna located ~ 6 km from the array center was discarded during the reduction stage since no flux could be seen in the longest baselines. This left 10 baselines with the remaining 5 antennas which spanned a baseline range of 61m to 459m. With this configuration it is possible to detect structures up to $\sim 22'$. With the ATCA 22m antennae, the FWHM of the primary beam is $\sim 33'$. The mean system temperature during the run was $T_{sys} \simeq 35$ K. A bandwidth of 7.4 MHz was used with a channel spacing of 7.8 kHz, for a velocity resolution of 1.65 km s^{-1} .

The synthesis data were edited and calibrated using the NRAO AIPS reduction software package. A bandpass calibration was applied using the PKS 0407–658 data and the continuum was subtracted by fitting a straight line to the real and imaginary parts of line-free channels in the UV plane and subtracting the fit from the data. The images were then computed using natural weighting for the UV data (higher weight to the shorter baselines) which gives maximum sensitivity while decreasing the spatial resolution by about a factor of 2. During the processing of generating the radio image, the data were also Hanning smoothed in velocity, thus decreasing the velocity resolution to 3.3 km s^{-1} . The full resolution data cube has a synthesized beam of $205'' \times 86''$ and an rms noise in each channel of 2.5 mJy/beam. The CLEANed data cube, restored with a synthesized beam of $240'' \times 240''$, has a noise of 3.3 mJy/beam. The channel maps of the cleaned data cube are shown in Figure 1. One can see already in these maps that

most of the detected signal is located away from the center of the image. As with the Parkes observations, the ACTA pointing corresponded to the optical centroid of Sculptor.

2.3. SEST CO Observations

Sculptor was observed with the SEST (Table 4) in the $J = 1 \rightarrow 0$ line emission of ^{12}CO at 115 GHz in January 1997. The Schottky receiver and good weather conditions yielded system temperatures averaging 370 K. The low-resolution Acousto Optical Spectrometer (LRS2) was used as the backend with a bandwidth of 1088 MHz and a frequency resolution of 1.4 MHz (3.6 km s^{-1}), centered on a heliocentric velocity of 110 km s^{-1} . A detailed description of SEST can be found in Booth et al (1989).

Antenna temperatures were calibrated using the chopper wheel method, and relative calibration uncertainties are estimated to be about 10%. The beamwidth at this frequency is $43''$. The observations were made in a double-beam-switching mode with a throw of $12'$ and a scan integration time of 120 seconds. Integrations were performed at five distinct locations on the galaxy, corresponding to the off-center HI peaks in both the NE and SW components, as well as on the inner edges of the HI clouds since this is very often where CO is detected in dE systems (see p.e. NGC 185 & NGC 205 in Young & Lo, 1997a). The spectra were co-added and smoothed in various ways to try to detect any CO emission, but regardless of the methods employed, no emission was found at any of these locations. Spectra of all the observed positions were then added together, yielding an average spectrum representing a total integration time of 15.5 hours, with a rms noise level of 2.1 mK. The 3σ CO brightness temperature limit is therefore $T_{mb} < 9.0 \text{ mK}$, after beam efficiency corrections (taking $\eta_{mb} = 0.7$ for the SEST at 115 GHz), corresponding to a CO integrated intensity $I_{CO} = \int T_{mb} dV < 0.2 \text{ K km s}^{-1}$.

3. ANALYSIS OF THE HI DATA

3.1. HI Content

Figure 2 shows the average spectrum of the 100 minute Parkes integration at the central position of Sculptor. From it, a systemic velocity of $112 \pm 3 \text{ km s}^{-1}$ was derived, very close to the optical velocity of $110 \pm 1.4 \text{ km s}^{-1}$. The detected flux of 5.7 Jy translates into an HI mass of $\sim 1.0 \times 10^4 \text{ M}_\odot$ at

the distance of Sculptor. Since, as will be seen below, a large fraction of the HI probably lies outside the HPBW of the Parkes beam, this mass estimate should only be considered as a lower limit of the total HI content of Sculptor.

Figure 3 shows the global profile from the ATCA observations. Notice that the systemic velocity from this spectrum is slightly different from the Parkes spectrum: $102 \pm 5 \text{ km s}^{-1}$. This already suggests that a considerable fraction of the gas detected by the synthesis observations is different from the gas seen in the the single dish observation. This can be seen more clearly in Figure 4 where the two spectra have been superposed. The integrated ATCA profile gives a total detected flux of $17.3 \text{ Jy km s}^{-1}$, which implies a total detected HI mass of $3.0 \times 10^4 \text{ M}_\odot$ at the adopted distance of Sculptor.

3.2. HI Distribution

Figure 5 shows the HI surface density map for the gas detected by the synthesis observation. It can be seen that most of the HI is located within two distinct clouds located $15' - 20'$ from the optical center. It is quite likely that a large fraction of the gas present in this map was not detected in our single dish observations with the $14.9'$ Parkes beam centered at the optical position. Moreover, a large fraction of the gas is also outside the HPBW of the primary beam ($\sim 33'$) of the ATCA antennae; thus, even if the data in Figure 5 were corrected for primary beam attenuation, this single field observation will have missed any gas located further out from the center of the galaxy. Given the observed distribution of gas in Sculptor, it is at least plausible, and we believe probable, that more extended HI gas is present.

There is also another reason (already mentioned in Sec. 2.2) which suggests that this observation may not have detected all the flux present. The diameter of the detected clouds is $\sim 20'$ which is close to the largest structures ($\sim 22'$) that can be detected with the shortest baseline ($\sim 60\text{m}$) of the 375m ACTA configuration we employed. Shorter baselines are needed to detect larger structures if they exist. Thus, the $3.0 \times 10^4 \text{ M}_\odot$ of HI detected within the primary beam by the ATCA observation should also be considered as a lower limit. Another indication that the ATCA observations has not detected all the flux can be seen in Figure 4 which shows that there is some flux seen around 125 km s^{-1} in the single dish observations that is not seen in the interferometric data.

The fact that most of the H I sits at the edge of the optical component of Sculptor is illustrated even more clearly by the H I radial profile shown in Figure 6. This distribution is reminiscent of what has been observed in some extreme dIrr systems. In their 1994 paper, Puche and Westpfahl summarized the situation in low mass systems such as Sextans A, Holmberg I and M81dwA as follows:

“Very little gas remains in the central regions of the galaxies. The inner limit of the H I shell nearly coincides with the optical radius of the galaxy. The outer extent of the H I shell is about 1.5 times the optical radius.”.

This is a nearly perfect description of what we have observed in Sculptor, though a complete H I shell has not yet been mapped.

3.3. HI Kinematics

The map of the isovelocity contours for the detected H I is showed in Figure 7. The mean radial velocities for the 3 clouds are $98 \pm 8 \text{ km s}^{-1}$ for the NE cloud, $119 \pm 2 \text{ km s}^{-1}$ for the central cloud and $104 \text{ km s}^{-1} \pm 11$ for the SW cloud. It is difficult to determine conclusively whether the H I clouds are in rotation around the main body of the galaxy. This might be surprising since no hint of rotation has been found in any dSph systems that have adequate data (Mateo 1994) with the exception maybe of Ursa Minor (Hargreaves et al. 1994). It is equally difficult to determine with any certainty whether the clouds in Sculptor are systematically expanding or contracting from or towards the galaxy center. What makes the interpretation of the kinematical data difficult is that we have no independent constraint on the true orientation parameters of the galaxy and even less on the origin or orientation of the gas. The various different possibilities will be discussed in the next section.

The H I velocity dispersion map is shown in Figure 8. The mean dispersions for the three clouds are $4.3 \pm 2.5 \text{ km s}^{-1}$ for the NE cloud, $2.3 \pm 1.2 \text{ km s}^{-1}$ for the central cloud and $3.8 \pm 2.2 \text{ km s}^{-1}$ for the SW cloud with the exception of a small region (dark area around $00^{\text{h}} 59^{\text{m}} 30^{\text{s}}$ and $-33^{\circ} 52' 00''$) where $\langle \sigma \rangle \simeq 15 \pm 2 \text{ km s}^{-1}$. While the mean velocity dispersion $\sim 4 \pm 2 \text{ km s}^{-1}$ of the gas in the outer parts appears to be smaller than the stellar velocity dispersion $\sim 6 \pm 1 \text{ km s}^{-1}$ observed in the center (Armandroff and Da Costa

1986; Queloz et al 1995), they are still comparable within the quoted errors.

4. DISCUSSION

In trying to understand the properties of the ISM in Sculptor, we must try to reconcile the following principal characteristics of the galaxy and its relation to the Milky Way. First, Sculptor is presently located relatively close to the Milky Way, and its perigalactic distance is even closer ($\sim 60 \text{ kpc}$; Irwin and Hatzidimitriou 1995; Schweizer et al 1995). Consequently, it is possible (see sec. 4.2) that tidal effects have played some role in producing the observed distribution of gas in the galaxy. This may help reconcile why gas that may be of an internal origin, is located so close to the edge of the optical image of the galaxy. Because Sculptor is relatively close, one must also carefully consider the possibility that the detected gas may not be associated with Sculptor but is instead a high-velocity cloud from the Magellanic Stream or some other complex that happens to be present in this part of the sky.

4.1. Internal Origin

Is it possible to account for the neutral gas seen in Sculptor from mass loss in normal giants? The most likely internal sources of gas that can be realistically retained in the vicinity of Sculptor are winds from evolved stars on the red-giant and asymptotic giant branches, and gas expelled during the planetary nebula phase of intermediate-age and old stars. Since the central regions of dSph galaxies appear to be devoid of neutral gas (Knapp et al 1978; Mould et al 1990; Koribalski et al 1994; this paper), and since they reveal no obvious signs of dust or molecular gas (with the exceptions of NGC 185 and NGC 205, both of which are sometimes considered ultra-luminous dSph systems; Young and Lo 1997a; Mateo 1998), a supernova would eject most, if not all, of the existing gas from a galaxy as small as Sculptor (Mac-Low and Ferrara 1998) as well as its own ejecta. Any supernovae would simply complicate the gas-retention problem; if a galaxy such as Sculptor is to retain gas from internal sources, the more sedate (and slow) sources of gas must dominate the generation of the ISM.

As summarized by Mould et al (1990), the total mass loss rate expected from normal evolution is about $0.015 \text{ M}_\odot \text{ yr}^{-1}$ per $10^9 \text{ L}_\odot, B$. For Sculptor ($L_B \sim 10^7 \text{ L}_\odot$, Mateo 1998), this implies a total

return of $1.5 \times 10^5 M_{\odot}$ per Gyr. At this rate, it would take ~ 200 Myr to produce the observed amount of H I seen in Sculptor even if all of the ejected gas is retained by the galaxy and is converted to neutral H, neither of which is probably correct. If we assume that the mass distribution in Sculptor is more extended than the light (Da Costa 1994), the escape velocity may be as much as 3.0 times larger than the central dispersion of 6.6 km/s, or about 20 km/s, or may be as only about twice the central dispersion, or about 13 km/s, if the mass follows the light distribution. The velocity spectrum of red giant winds extends somewhat above even this upper limit, suggesting that up to 80% of the gas from such winds can be lost from the galaxy. Thus, the rejuvenation time of the ISM from internal sources must be considerably longer than 200 Myr.

For our purposes, the key point is that it should take from 200–1000 Myr to build up the amount of gas seen in Sculptor, and even longer if a significant fraction of the gas is in molecular form (observations of dE's suggest that there could be as much mass in H₂ than in H I ; Wiklind, Combes & Henkel 1995). Since most of the SF seems to have taken place between 8 and 10 Gyr in Sculptor (Da Costa 1984), it would have produced a gas reservoir of $\sim 3.0 \times 10^5 M_{\odot}$. So, only 10% of this need to be retained in its neutral form to account for the H I detected by the present observations.

Of course, for other dSph galaxies in which H I is not detected, these same arguments should apply; for these systems the problem shifts to how the gas is lost or is otherwise made unobservable. Galaxies such as Fornax (Stetson 1997; Demers et al 1998) and Carina (Smecker-Hane et al 1994; Mighell 1997; Hurley-Keller et al 1998), which show clear evidence of SF episodes even within the last few Gyr, show as yet *no* evidence of neutral gas, at least in the central regions. In these cases, perhaps there simply has not been enough time to generate a reservoir of gas. But what about Ursa Minor, Draco, Sextans, and Leo II? These galaxies contain no significant populations younger than the youngest stars found in Sculptor. If Sculptor could retain gas from red giants and planetary nebulae, why didn't these? Have we looked at the right place?

4.2. Tidal Effects

Another possibility is that the gas was removed from the outer parts of Sculptor by tidal forces from

the Milky Way during its last perigalactic passage $\sim 10^8$ years ago (Irwin and Hatzidimitriou 1995). This idea is based on the fact that while the central 10 arcmin of Sculptor (i.e. the optical core) has zero ellipticity, outside this region, the ellipticity smoothly increased to the asymptotic value of ~ 0.3 (Irwin and Hatzidimitriou 1995). This picture is similar to numerical simulations of dSph galaxies that are tidally disrupted where material is ejected ahead of and behind the satellite (eg, Allen and Richstone 1988; McGlynn & Borne 1991; Moore and Davis 1994; Piatek and Pryor 1995; Oh et al 1995; Kroupa 1997). Is it a coincidence that the position angle of the proper motion measured by Schweitzer et al (1995) of $40^{\circ} \pm 24^{\circ}$ happens to be almost exactly the position angle defined by the two H I clouds (see Figure 5)? Tidal effects could produce two clouds symmetrically distributed on both sides of the optical center. Moreover, when stars (and gas) are detached from the host galaxy, they continue to follow their host's galactic orbit for several galactic years before dispersing beyond the host's tidal radius (Oh et al 1994).

With few exceptions, the dSph galaxies of the Local Group are clustered around the MW and M31, while the dIrr galaxies are more evenly distributed throughout the group (Mateo 1998). This certainly suggests that the proximity of a massive galaxy may have played an important role in determining the structural and kinematic properties of dSph systems. The removal of their gas by tidal effects may be one of the important results of these encounters, though whether this can explain our observations of Sculptor remains unclear.

4.3. Gas Falling Back or Expanding ?

A number of authors have at various times suggested that dSph systems may be the remnants of extremely low-luminosity dIrr galaxies that have been depleted of gas by their initial or subsequent SF episodes, or perhaps by tidal effects (eg, Ferguson and Binggeli 1994; but also see Mateo 1998 and references therein). This scenario is supported by the fact that large expanding cavities surrounded by dense shells are found in the neutral interstellar medium of many dIrr galaxies that were observed with sufficient resolution (Puche and Westpfahl 1994). The energetics of the gas suggest that these structures are plausibly created by stellar winds and supernova explosions from the young dIrr stellar populations (Larson 1974, Dekel & Silk 1986).

The largest dwarfs, such as Magellanic irregular systems (e.g. IC 2574, Martimbeau, Carignan and Roy 1994; Holmberg II, Puche et al. 1992), contain several such shells. However, in the smallest dwarfs (e.g. Holmberg I and M81dwA, Westpfahl and Puche 1994; Leo A, Young and Lo 1996), only one large slowly ($v_{exp} \simeq 5 \text{ km s}^{-1}$) expanding shell usually dominates the ISM. The expansion and contraction of the entire ring- or shell-like ISM of these small galaxies is interpreted as being the result of burst(s) of SF that took place in those systems.

dSph systems, such as Sculptor, are in the same mass range than the low luminosity dIrr galaxies ($M_B \simeq -10$) and a similar process may have taken place. Soon after the primordial burst of SF, most of the ISM could have been expelled from the inner regions of the galaxy by stellar winds and supernova explosions, stopping SF. Depending on the energy released in the initial burst, and the total mass of the system, some of the gas may be falling back into the galaxy, giving the H I a ring-like appearance. The ring size would depend on the parent galaxy mass, the strength of the initial burst and time. In the case of Sculptor, because of the missing short spacings of the present observations which do not allow to see structures larger than $\sim 22'$, it is possible that we are only seeing the two regions of highest surface density. Perhaps most difficult for this interpretation is the lack of any obvious, recent stellar population that may have ejected the gas. As in the tidal scenario, we must suppose that the gas, if ejected by SF processes, has been able to stay associated with Sculptor and remain in the outer parts of the galaxy since its last burst.

The H I gas observed in a galaxy like Phoenix could have another origin. Van de Rydt, Demers and Kunkel (1991) found that this system has an intermediate population of blue stars with an age of $\sim 1.5 \times 10^8$ years along with an old, globular cluster-like population. If that last burst of SF is responsible for the observed H I location, and if we assume a constant expansion velocity of 5 km s^{-1} (as estimated in extreme low mass dIrr systems), most of it should be found around $\sim 750 \text{ pc}$ ($\Delta \simeq 400 \text{ kpc}$), which corresponds to $\sim 6.5'$ on the sky. In recent VLA observations of Phoenix (Young & Lo 1997b), an H I “cloud” was found at about the right distance west of the center. However, it is difficult to know if that gas, detected at $\sim -23 \text{ km s}^{-1}$, is truly associated with Phoenix since no optical velocity is available.

If the same kind of calculations is applied to Sculptor, the radius where the H I is found would imply that the most recent burst of SF would have taken place $\sim 10^8$ years ago. Could the blue stars observed by Da Costa (1984) and Grebel et al (1994) around magnitudes 21 to 23 be the tip of such a population? The deepest existing CMD of Sculptor (Da Costa 1984) tells us that the most recent burst of SF in the galaxy occurred more than 5-8 Gyr ago, but these data are strictly from a small region near the center of Sculptor. Thus, while this scenario appears highly unlikely, deeper CMDs over a much larger portion of Sculptor are needed to determine if a recent burst of sufficient magnitude has occurred in this system. If such a population were found, it could potentially explain the location and amount of detected gas. If no young stars (or too few) are present, it becomes immediately more likely that if the observed H I came from an internal source, the gas had to have been produced during an initial burst of SF in Sculptor (then remained in the vicinity of the galaxy for nearly a Hubble time), or else slowly accumulated from giants winds and planetary nebulae as described above.

4.4. External Origin

A large H I cloud was recently detected near the distant dSph galaxy Tucana (Oosterloo et al 1996). Because the position of the cloud does not coincide too well with the optical galaxy and because the total gas mass inferred at Tucana's distance is rather large ($> 10^6 M_\odot$), these authors argued that the detected gas is more likely to be a HVC associated with the MS (Mathewson et al 1974). Could the same thing be happening with Sculptor? This is a reasonable possibility: Sculptor is close to the South Galactic Pole where the MS has a complex structure and several velocity components (Haynes and Roberts 1979). However, the highly symmetric distribution of the gas in Sculptor relative to the optical image of the galaxy, and the nearly perfect velocity correspondence between the radio and optical observations, suggest strongly that in Sculptor's case we are not dealing merely with an optical/radio illusion. Instead, the proximity of HVCs suggests that Sculptor may have actually accreted gas – or is in the process of doing so – from external clouds.

There is circumstantial evidence supporting the notion that dSph galaxies may be accreting gas of external origin. In Carina, Smecker-Hane et al (1994) argue for a large age spread yet a surprisingly small

spread in abundance. This is in striking contrast to Leo I which has a complex SF history (Lee et al 1993) and a broad giant branch indicative of a large abundance spread. This behavior makes somewhat more sense if the gas that formed distinct generations of stars in these galaxies was accreted or captured from distinct clouds with their individual – and therefore random – mean abundances. Wakker and van Woerden (1997) review the observations of HVC in the halo; their summary of past surveys suggest that many small, low-column density, and distant clouds could still be hidden throughout the Galactic halo.

The low velocity dispersions that makes it difficult for dwarfs to retain much of an ISM from internal sources also seems to limit the feasibility of capture from outside sources even more severely. The dispersion in the halo is 10–20 times higher than in dwarfs such as Sculptor, so very little gas could be captured in a random collision. The other possibility is that the galaxies and clouds follow more ordered motions. Lynden-Bell and Lynden-Bell (1995) have recently reviewed the possibility of kinematically and spatially related streams of objects in the Galactic halo; they conclude that some such streams may exist, but Sculptor in particular does not seem to be associated with any stream containing any other galaxies or halo clusters. Indeed, a measurement of the proper motion of Sculptor (Schweitzer et al 1995) seems to rule out its association with all previously identified galaxy streams. Nonetheless, these results do not rule out that Sculptor may be located in a stream of H I clouds – the lack of distance information for the clouds makes it impossible to constrain the existence of such streams. If galaxies such as Sculptor (and Carina, Fornax, and Leo I when they were forming stars) did in fact accrete gas from an external source, this would seem to be the only way – contrived as it is – of doing so.

5. SUMMARY AND CONCLUSIONS

We have obtained Parkes single dish and ATCA synthesis observations of the Sculptor dSph galaxy and have clearly detected H I associated with this galaxy. Our principal results include:

- (1) The single dish observation has detected $1.0 \times 10^4 M_{\odot}$ of H I at a systemic velocity of $112 \pm 3 \text{ km s}^{-1}$, which is similar to the mean velocity of the stellar component.
- (2) The synthesis observation allows to set a lower

limit to the total H I content of $3.0 \times 10^4 M_{\odot}$. The mean velocity of the gas detected with the ATCA is $102 \pm 5 \text{ km s}^{-1}$.

(3) Most of the detected gas is located in two clouds symmetrically distributed $15' - 20'$ to the NE and SW of the optical center. This distribution and good velocity coincidence with the optical component of Sculptor virtually guarantees that the gas is truly associated with the galaxy.

(4) The fact that a large fraction of the detected H I is outside the $33'$ HPBW of the ATCA antennas and that the sizes of the detected H I clouds ($\sim 20'$) are close to the theoretical largest structures ($\sim 22'$) that can be seen by the 375 m array configuration, suggest that much more H I may be present in Sculptor but were missed by the present observations. The masses derived from the interferometric observations should thus be considered as lower limits.

(5) The amount of H I detected is $\sim 10\%$ of the estimated mass loss from normal giants during its main epoch of SF 8–10 Gyr ago.

(6) Tidal effects due to the proximity of the MW may have played a role in the observed distribution of the gas.

(7) The detected H I could be either gas expelled in the original burst of SF that is falling back onto the system or gas expelled in a more recent burst of SF that would have taken place $\sim 10^8$ years ago. However, since there is as yet no clear evidence for such a young stellar population in Sculptor, the first alternative is only reasonable if there is a way for the gas to have remained in the vicinity of Sculptor for most of the galaxy's lifetime.

(8) If the gas is of an external origin, one must provide a model where a low-mass galaxy such as Sculptor can acquire gas from such a hot system as the Galactic halo. Because the velocity difference of Sculptor and the Magellanic Stream is $\sim 125 \text{ km s}^{-1}$ in this part of the sky, it is very likely that the detected H I did not derive from that source of gas, but possibly from some other unidentified or now-defunct stream. In any case, the gas is almost certainly not merely a component of the MS that is seen in projection about the optical component of Sculptor.

Table 5 compares the properties of the dSph systems to other Local Group dIrr and dE systems. Looking at (M_{HI}/L_V) it can be seen that Sculptor and Phoenix appear to have about 10 times more H I than has been detected in the dE companions

of M31 and about 40 to 150 times less H I than what is seen in dIrr galaxies having similar absolute magnitudes. In the case of the dE galaxies, the H I detected is relatively close to the center. It is possible that more H I is present at larger radii. In the case of Sculptor and Phoenix, the H I masses are clearly lower limits. It is possible that mapping larger areas around those systems will reveal a much larger quantity of gas. If this is the case, this would lend support to the suggestion that some dSph systems may be remnants of extreme dIrr galaxies which have been stripped of their gas by tidal effects or SF bursts. If this stripping/ejection scenario is correct, H I should also be observed at large radii in the other dSph systems. Since the observations used to derived the upper limits given in Table 5 were centered on the optical images of the galaxies, it remains entirely possible that other dSph systems contain large quantities of neutral gas that has so far escaped detection.

We would like to thank the staff of the Parkes and ATCA facilities for their support during the HI data acquisition, James Lequeux for his help in planning the SEST observations, and Tommy Wiklind for his support during the CO observations. CC & SD acknowledge grants from NSERC.

REFERENCES

Aaronson, M. 1986, in *Stellar Populations*, eds C.A. Norman, A. Renzini & M. Tosi (Cambridge: Cambridge University Press), p. 45

Aaronson, M., & Olszewski, E.W. 1987, AJ, 94, 657

Allen, A.I. & Richstone, D.O. 1988, ApJ, 325, 583

Armandroff, T.E., & Da Costa, G. 1986, AJ, 92, 777

Booth, R.S., Delgado, G., Hagstrom, M., Johansson, L.E.B., Murphy, D.C., Ilberg, M., Whyborn, N.D., Greve, A., Hansson, B., Lindstrom, C.O., & Rydberg, A. 1989, A&A, 216, 315

Canterna, R., & Flower, P.J. 1977, ApJ, 212, L58

Carignan, C., Beaulieu, S., & Freeman, K.C. 1990, AJ, 99, 178

Carignan, C., Demers, S., & Côté, S. 1991, ApJ, 381, L13

Da Costa, G. 1984, ApJ, 285, 483

Da Costa, G. 1988, in *The Harlow Shapley Symposium on Globular Cluster Systems in Galaxies*, eds J.E. Grindlay & A.G. Davis Philip (Dordrecht: Reidel), p. 217

Da Costa, G. 1994, in *ESO/OHP Workshop on Dwarf Galaxies*, eds G. Meylan & P. Prugniel (ESO: Garching), p. 221

Dekel, A., & Silk, J. 1986, ApJ, 303, 39

Demers, S., Mateo, M., & Kunkel, W.E. 1998, AJ, in press

de Vaucouleurs, G., de Vaucouleurs, A., Corwin, H.G., Buta, R.J., Paturel, G., & Fouqué, P. 1991, *Third Reference Catalogue of Bright Galaxies* (Springer-Verlag)

Ferguson, H.C., & Binggeli, B. 1994, A&A Rev., 6, 67

Grebel, E.K., Roberts, W.J., & van de Rydt 1994, in *CTIO/ESO Workshop on The Local Group: Comparative and Global Properties*, eds A. Layden, R.C. Smith & J. Storm (ESO: Garching), p. 148

Hargreaves, J.C., Gilmore, G., Irwin, M.J., & Carter, D. 1994, MNRAS, 271, 693

Haynes, M.P., & Roberts, M.S. 1979, ApJ, 227, 767

Hurley-Keller, D., Mateo, M., & Nemec, J. 1998, AJ, in press

Ibata, R.A., Gilmore, G., & Irwin, M.J. 1995, MNRAS, 277, 781

Irwin, M.J., Bunclark, P.S., Bridgeland, M.T., & McMahon, H.G. 1990, MNRAS, 244, 16p

Irwin, M., & Hatzidimitriou, D. 1995, MNRAS, 277, 1354

Johnson, D. W., & Gottesman, S. T. 1983, ApJ, 275, 549

Kaluzny, J., Kubiak, M., Szymmański, M., Udalski, A., Krzeminiński, W., & Mateo, M. 1995, A&AS, 112, 407

Koribalski, B., Johnston, S., and Otrupcek, R. 1994, MNRAS, 270, L43

Knapp, G.R., Kerr, F.J., & Bowers, P.F. 1978, AJ, 83, 360

Kroupa, P. 1997, New Astronomy, 2, 139

Larson, R.B. 1974, MNRAS, 169, 229

Lee, M.G., Freedman, W., Mateo, M., Thompson, I., Roth, M., & Ruiz, M.T. 1993, AJ, 106, 1420

Lynden-Bell, D., & Lynden-Bell, R.M. 1995, MNRAS, 275, 429

MacLow, M.-M., & Ferrara, A. 1998, astro-ph/9801237

Martimbeau, N., Carignan, C., & Roy, J.-R. 1994, AJ, 107, 543

Mateo, M. 1994, in ESO/OHP Workshop on Dwarf Galaxies, eds G. Meylan & P. Prugniel (ESO: Garching), p. 309

Mateo, M. 1998, ARA&A, in press

Mathewson, D., Cleary, M.N., & Murray, J.D. 1974, ApJ, 190, 291

McGlynn, T.A., & Borne, K.D., 1991, ApJ, 372, 3

Mighell, K.J. 1997, AJ, 114, 1458

Moore, B. & Davis, M. 1994, MNRAS, 270, 209

Mould, J.R., Bothun, G.D., Hall, P.J., Staveley-Smith, L., & Wright, A.E. 1990, ApJ, 362, L57

Oh, K.S., Lin, D.N.C., & Aarseth, S.J. 1994, in ESO/OHP Workshop on Dwarf Galaxies, eds G. Meylan & P. Prugniel (ESO: Garching), p. 381

Oh, K.S., Lin, D.N.C., & Aarseth, S.J. 1995, ApJ, 442, 142

Oosterloo, T., Da Costa, G.S., & Staveley-Smith, L. 1996, AJ, 112, 1969

Ortolani, S., & Gratton, R.G. 1988, PASP, 100, 1405

Piatek, S. & Prior, C. 1995, AJ, 109, 1071

Puche, D., & Westpfahl, D. 1994, in ESO/OHP Workshop on Dwarf Galaxies, eds G. Meylan & P. Prugniel (ESO: Garching), p. 273

Puche, D., Westpfahl, D., Brinks, E., & Roy, J.-R. 1992, AJ, 103, 1841

Queloz, D., Dubath, P., & Pasquini, L. 1995, A&A, 300, 31

Sargent, W.L.W., Sancisi, R., & Lo, K.Y. 1983, ApJ, 265, 711

Schweitzer, A.E., Cudworth, K.M., Majewski, S.R., & Suntzeff, N.B. 1995, AJ, 110, 2747

Skillman, E.D., Terlevich, R., Teuben, P.J., & van Woerden, H. 1988, A&A, 198, 33

Smecker-Hane, T.A., Stetson, P.B., Hesser, J.E., & Lehnert, M.D. 1994, AJ, 108, 507

Stetson, P.B. 1997, Baltic Ast., 6, 3

Thuan, T.X. & Martin, G.E. 1979, ApJ, 232, L11

van de Rydt, F., Demers, S., & Kunkel, W.E. 1991, AJ, 102, 130

van den Berg, S. 1994, ApJ, 428, 617

Wakker, B.P., & van Woerden, H. 1997, ARA&A, 35, 217

Westpfahl, D., & Puche, D. 1994, in ESO/OHP Workshop on Dwarf Galaxies, eds G. Meylan & P. Prugniel (ESO: Garching), p. 295

Whiting, A.B., Irwin, M.J., & Hau, G.K.T. 1997, AJ, 114, 996

Wiklind, T., Combes, F., & Henkel, C. 1995, A&A, 297, 643

Young, L.M., & Lo, K.Y. 1996, ApJ, 462, 203

Young, L.M., & Lo, K.Y. 1997a, ApJ, 476, 127

Young, L.M., & Lo, K.Y. 1997b, ApJ, 490, 710

TABLE 1
PHYSICAL PARAMETERS OF SCULPTOR.

Morphological Type	dSph
RA (J2000.0) ^a	01 ^h 00 ^m 09 ^s 4
Dec (J2000.0) ^a	-33°42'33"
l ^a	287°53'
b ^a	-83°16'
Galactocentric distance ^b	87.5 ±6 kpc (1' ≈ 25.5 pc)
Isophotal major diameter, D ₂₅ ^a	40'
Core radius, r _c ^c	5.8 ±1.6
Tidal radius, r _t ^c	76.5 ±5.0
Major axis PA ^c	99° ±1°
Proper motion PA ^d	40° ± 24°
Abundances [Fe/H] ^b	[-2.2, -1.6]
Absolute magnitude, M _B ^a	-10.0
Total luminosity, L _B	1.5 × 10 ⁶ L _⊙
Absolute magnitude, M _V ^e	-10.7
Total luminosity, L _V	1.6 × 10 ⁶ L _⊙
Optical velocity, V _⊙ ^e	110 ± 1.4 km s ⁻¹
Galactocentric velocity, V _{GSR}	77 km s ⁻¹

^ade Vaucouleurs et al. (1991).

^bKaluzny et al. (1995).

^cIrwin & Hatzidimitriou (1995).

^dSchweitzer et al. (1995).

^eQueloz, Dubath & Pasquini (1995).

TABLE 2
PARAMETERS OF THE PARKES HI OBSERVATIONS.

Dates of observations	1992 January 25–30
Flux calibrator	PKS 1934–638
System temperature, T_{sys}	~50 K
Primary beam at half-power (FWHM)	14.9 ± 0.2
Bandwidth	8.0 MHz
Central velocity	300 km s^{-1}
Velocity range	$[-544, 1144] \text{ km s}^{-1}$
Channel width	7.8 kHz (1.65 km s^{-1})

TABLE 3
PARAMETERS OF THE ATCA HI OBSERVATIONS.

Date of observations	1992 October 2
Integration time on source	8.2 hours
Configuration	375 m.
Baselines	10 [61m, 459m]
Flux calibrator	PKS 0407–658
Phase calibrator	PKS 0042–442
System temperature, T_{sys}	~35 K
Primary beam at half-power (FWHM)	$33'$
Bandwidth	7.4 MHz
Channel spacing (no smoothing)	7.8 kHz (1.65 km s^{-1})
Channel spacing (after Hanning smoothing)	15.6 kHz (3.3 km s^{-1})
FWHM of synthesized dirty beam	$205'' \times 86''$
FWHM of restored cleaned beam	$240'' \times 240''$
RMS noise in channel maps (full resolution / no cleaning)	2.5 mJy/beam
RMS noise in channel maps (after cleaning / convolved)	3.3 mJy/beam
Conversion factor, $240'' \times 240''$ beam (equivalent to 1 mJy/beam area)	0.01 K
Maps gridding	$30'' \times 30''$ pixels

TABLE 4
PARAMETERS OF THE SEST CO OBSERVATIONS.

Dates of observations	1997 January 24–29
System temperature, T_{sys}	370 K
Primary beam at half-power (FWHM)	43''
Bandwidth	1088 MHz
Central velocity	110 km s^{-1}
Velocity range	[-1300, 1500] km s^{-1}
Channel width	1.4 MHz (3.6 km s^{-1})

TABLE 5
HI IN LOCAL DSPH'S, DI'S & DE'S.

Name	M_V^a	R_{GC}^a (kpc)	L_{tot} (L_V) $_{\odot}$	\mathcal{M}_{HI} (\mathcal{M}_{\odot})	(\mathcal{M}_{HI}/L_V) (\mathcal{M}/L_V) $_{\odot}$	ref.s
Fornax	-13.0	120	1.4×10^7	$< 10^4$...	(1)
Leo I	-11.5	198	3.4×10^6	$< 10^4$...	(1)
Sculptor	-10.7	87.5 ^b	1.6×10^6	$\geq 3.0 \times 10^4$	0.02	(2)
<i>Phoenix</i>	-9.9	≤ 400	7.6×10^5	1.0×10^5	0.07	(3)
Leo II	-9.6	207	5.9×10^5	$< 10^4$...	(1)
<i>Tucana</i>	-9.5	≤ 900	5.3×10^5	1.5×10^6	$\sim 3 ?$	(4)
Sextans	-9.2	83	4.1×10^5	< 130	...	(5)
Carina	-8.6	85	2.4×10^5	$< 10^3$...	(6)
Ursa Minor	-8.4	64	2.0×10^5	< 280	...	(1)
Draco	-8.3	72	1.8×10^5	< 68	...	(1)
Sagittarius	...	16 ^c
<i>Antlia</i>	...	1150 ^d
<hr/>						
Leo A	-13.9	2200	5.3×10^7	8.1×10^7	1.5	(7)
Sextans A	-13.8	1320	4.8×10^7	5.8×10^7	1.2	(8)
M81dwA	-11.0	3250	3.6×10^6	1.1×10^7	3.0	(9)
G.R. 8	-10.6	1100	2.6×10^6	2.0×10^7	0.8	(10)
<hr/>						
NGC 205	-15.7	850	1.6×10^8	4.3×10^5	0.003	(11)
NGC 185	-13.8	600	2.8×10^7	1.0×10^5	0.004	(11)
<hr/>						

^aIrwin & Hatzidimitriou (1995).

^bKaluzny et al. (1995).

^cIbata, Gilmore & Irwin (1995).

^dWhitting, Irwin & Hau (1997).

REFERENCES.—(1) Knapp, Kerr & Bowers 1978; (2) this paper (ATCA); (3) Carignan, Demers & Côté 1991; (4) Oosterloo, Da Costa & Staveley-Smith 1996; (5) this paper (Parkes); (6) Mould et al. 1990; (7) Young & Lo 1996; (8) Skillman et al. 1988; (9) Sargent, Sancisi & Lo 1983; (10) Carignan, Beaulieu & Freeman 1990; (11) Young & Lo 1997a

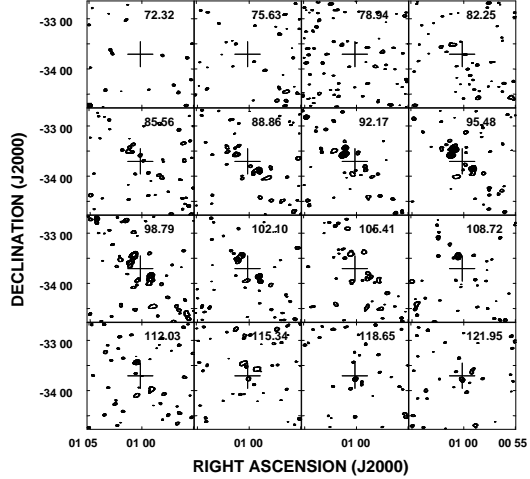


Fig. 1.— Channels maps from the AT observations. The levels are -0.1, 0.1, 0.2, 0.3, 0.4 & 0.5 K. The synthesized beam is shown in the bottom left corner of the first channel. The velocity of each channel is given at the top right corner. The cross in the center is $30' \times 30'$.

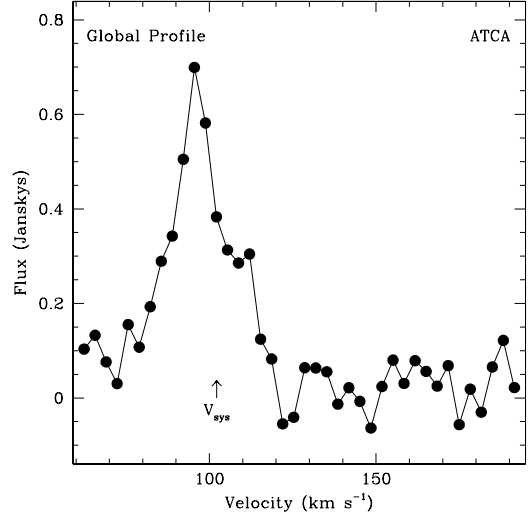


Fig. 3.— Global profile from the AT synthesis observations. From this profile, one gets $V_{sys} = 102$ km s^{-1} and $\mathcal{M}_{HI} \simeq 3 \times 10^4 \mathcal{M}_{\odot}$.

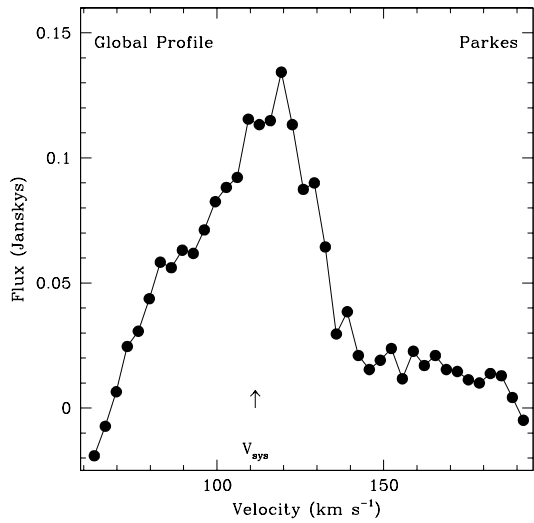


Fig. 2.— Global profile from the single dish Parkes observations. From this profile, one gets $V_{sys} = 112$ km s^{-1} and $\mathcal{M}_{HI} \simeq 1 \times 10^4 \mathcal{M}_{\odot}$.

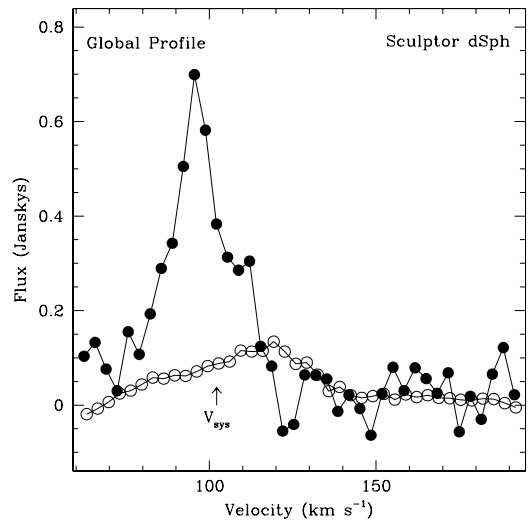


Fig. 4.— Global profile derived from the Parkes observations superposed on the global profile obtained from the AT observations.

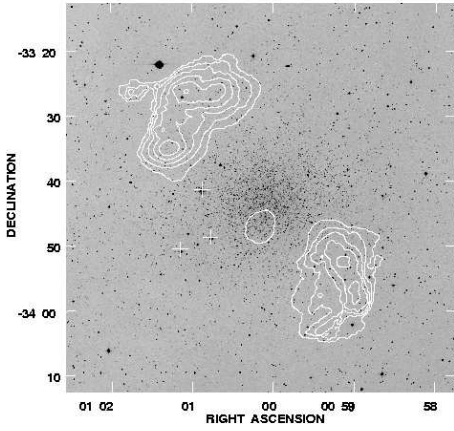


Fig. 5.— HI surface densities superposed on the STScI Digitized Sky Survey optical image. The contours are $0.2, 0.6, 1.0, 1.4, 1.8$ & $2.2 \times 10^{19} \text{ cm}^{-2}$. The data have been corrected for the primary beam attenuation.

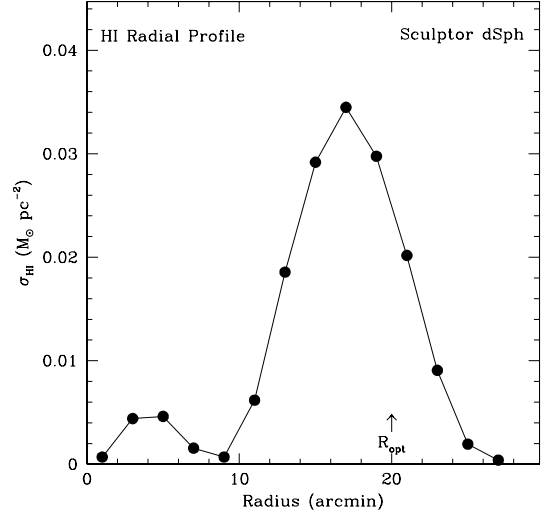


Fig. 6.— HI surface density radial profile. The optical size (R_{opt}) is indicated.

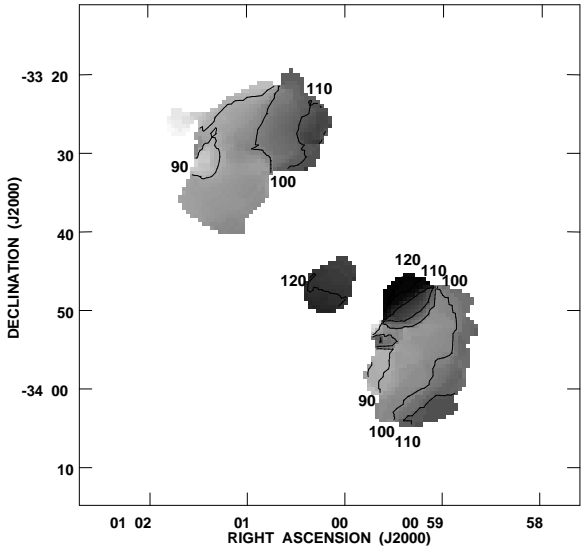


Fig. 7.— Velocity field map. The contours are $90, 100, 110, 120 \text{ km s}^{-1}$.

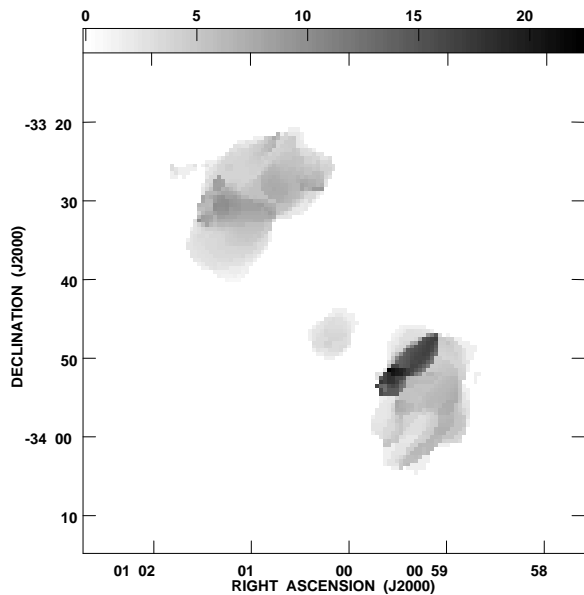


Fig. 8.— Velocity dispersion map. The velocity dispersion of the gas is almost everywhere less than 10 km s^{-1} . The mean dispersion is $\langle \sigma \rangle \simeq 2.3 \pm 1.2 \text{ km s}^{-1}$ in the central cloud and $\langle \sigma \rangle \simeq 4.1 \pm 2.3 \text{ km s}^{-1}$ in the NE & SW clouds with the exception of a region of high σ ($\langle \sigma \rangle \simeq 15 \pm 2 \text{ km s}^{-1}$) in the SW cloud.